



Islamic Azad University  
Mashhad Branch

# Prospection of Iron and Manganese Using Index Overlay and Fuzzy Logic Methods in Balvard 1:100,000 Sheet, Southeastern Iran

Misagh Mirzaei<sup>1\*</sup>, Peyman Afzal<sup>2</sup>, Ahmad Adib<sup>1</sup>, Masoumeh Khalajmasoumi<sup>3</sup>  
and Afshar Zia Zarifi<sup>4</sup>

1. Department of Mining Engineering, South Tehran Branch, Islamic Azad University, Tehran, Iran

2. Camborne School of Mines, University of Exeter, Penryn, UK

3. Department of Geology, Sciences and Research Branch, Islamic Azad University, Tehran, Iran

4. Department of Mining Engineering, Lahijan Branch, Islamic Azad University, Lahijan, Iran

Received 16 December 2013; accepted 10 February 2014

## Abstract

The focus of this study is the prospecting of iron and manganese in the Balvard 1:100,000 Sheet, situated in the Sanandaj - Sirjan Structural Zone, utilizing Index Overlay and Fuzzy Logic methods in the GIS. In this study, the layers for integration, alterations, geological, geophysical, geochemical and structural data are based on stream sediments, airborne magnetometric and remote sensing studies. Based on the results obtained by these methods, Fe and Mn prospects exist in both the Northern and Northeastern parts of the area. The prospect areas derived via the Fuzzy Logic method are larger than those derived from the Index Overlay method because the method used a range value from 0 to 1.

**Keywords:** Index overlay, Fuzzy logic, Prospecting, Balvard.

## 1. Introduction

The Geographic Information System (GIS) is a georeferencing system used in mineral exploration which provides an appropriate environment for importing, analyzing and modeling a large dataset considering that the selection of prospect areas in mineral exploration is a complex process and requires various criteria [1, 2]. In reconnaissance and prospecting studies, researchers can evaluate all of the digitized data in the different layers simultaneously. Digital geological mapping DGM in GIS can add the required spatial accuracy to the data, and also can enhance the versatility of the geological/structural map in many ways which are difficult to achieve through conventional mapping methods [3-7].

Different methods are used for integrating data layers in mineral explorations which are data-driven or based on conceptual models of mineralization and expertise for the determination of prospects (expert-based: [3, 4]). Index Overlay Model can be done in two ways. In both methods, first, weights are assigned to all of the effective factors based on their relative importance according to expert opinion. In the first method, the input factor maps are binary as in the Boolean method. In this method, each factor map has a single weight factor and is multiplied by its own weight factor and combined with other maps.

In the second method each of the input maps is allocated a weight as well as all classes and spatial units existing in each factor map based on its relative importance in conjunction with expert opinion. In other words, the different classes on a single map have different weights[8]. Moreover, the Fuzzy Logic technique has been used in ore mineralization prospecting, particularly in areas of detailed exploration [9,10]. In this study, the Index Overlay and the Fuzzy Logic methods were utilized for prospecting iron and manganese in the Balvard 1:100,000 Sheet, Southeastern Iran. The datasets consist of alterations, geological, structural, geochemical and geophysical layers in a GIS form.

## 2. Geographical and geological setting

The Balvard 1:100,000 Geological Sheets in Kerman Province, Southeastern Iran, are located in Sanandaj-Sirjan, a structural-metamorphic zone ([4]: Fig. 1). The Sanandaj-Sirjan Zone trends northwestward in western Iran on the Precambrian to Paleozoic basement and exposes abundant I-type granitoids and calc-alkaline volcanic rocks that were most active during the Late Jurassic to Upper Cretaceous periods [11,12]. The Nain-Baftophiolitic Belt (Central Iran) extends in a NW-SE direction in parallel with the Sanandaj-Sirjan Zone trend (Fig. 2). The main ultramafic massifs consist of harzburgites, small bodies of gabbros and dike swarm complexes, accompanied by various extrusives with composition basaltic-andesitic lava flows and breccias, dacites and

\*Corresponding author.

E-mail address (es): misagh\_mirzaei\_1@yahoo.com

rhyolites. The basaltic rocks of this belt include pegmatitic and isotropic gabbros, gabbroic–dibasic dykes, dyke swarm complex and pillow lavas. These massifs, to the north of the Mesozoic Magmatic Arc, crosscut the Sanandaj-Sirjan zone [13-15]. The ophiolite units are located in the Northeastern part of the area which is composed of ultramafic and mafic rocks (such as harzburgite and pridotite), capped by pelagic sediments resting directly on the ophiolite (Fig. 2: [15]). The Paleozoic units consisting of orthogneiss, muscovite, quartz, microcline and albite are present in the northern part of the sheet. Lower Cretaceous siltstones, fine-grained and coarse-grained stones, conglomerates and limestone-marl limestones are all located in the southern portion of the sheet [16]. There are several alterations consisting of chloritization, epidotization and carbonization. Rock units of Eocene volcanics including trachy andesite within the pyroclastic rocks occur in the Northeastern portion of the area (Fig. 2).

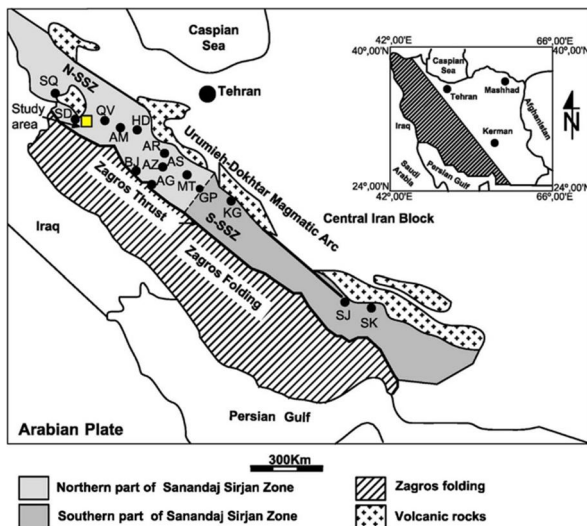


Fig.1. Distribution of major magmatic units in the Sanandaj-Sirjan zone, Zagros Orogen, (after [17], as modified by [12]). SQ – Saqqez, SD – Sanandaj, QV – Qorveh, AM – Almoghlagh, HD – Hamedan (Alvand), AR – Arak, AS – Astaneh, BJ – Boroujerd, AG – Aligudarz, AZ – Azna, MT – Muteh, KG – Koleh-Ghazi, SJ – Sirjan, SK – SiahKouh, GP – Golpaygan, N-SSZ and S-SSZ – north and south of the Sanandaj Sirjan Zone, respectively.

### 3. Methodology

Various models were used for real world events simulation in GIS environment [18]. Integration model was used for site selection by integrating related spatial data and effective criteria. There are various integration models that are categorized by their functions and their executive routines (Knowledge Driven or Data Driven). Knowledge Driven: The experience and knowledge of experts is used for executing models. Data Driven: Models are executed based on existent solutions and dependency value computation. We will

describe some of the models used in our application and mention our reasons for selecting them. These models consist of: Boolean Operation, Indexing Overlay, Fuzzy Logic and Genetic Algorithm.

Two methods were used in this study. They include the Index Overlay and the Fuzzy Logic methods which were used in combination with different informative layers, and processed using Arc Map 9.3 software. By comparing Index Overlay with Boolean Model's executive routines, it was apparent that the Index Overlay model had more flexibility as well as the ability to provide priority indication on spatial units of factor maps [19]. With respect to mentioned characteristics, this model is useful for comparing and evaluating integration models in the industrial estate site selection process [19].

#### 3.1. Index Overlay Method

In this method each map consists of various classes to which different values have been assigned; these values are multiplied by the pertinent weight, and the average score of each item (polygon or pixel) is computed. Then, these scores are added to the maps and combined. Finally, they are normalized by the sum of the weights. This method follows the general form below [20-22]:

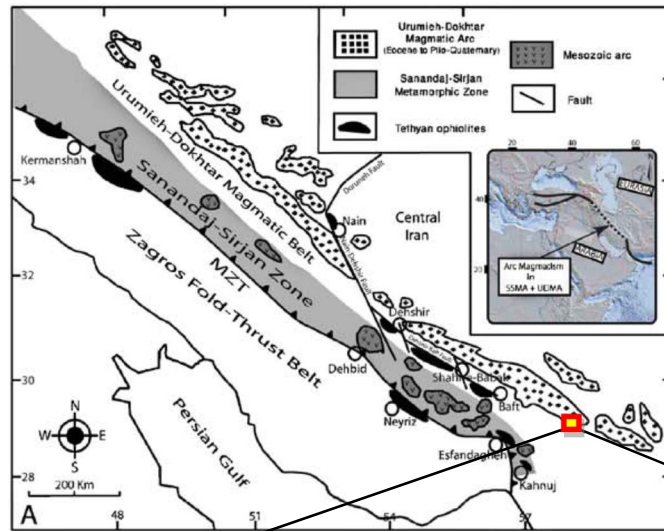
$$S = (\sum_i^n S_{ij} W_i) / (\sum_i^n W_i) \quad (1)$$

Where S denotes a weighted score for each condition  $W_i$  is the weight of  $i^{\text{th}}$  input map,  $S_{ij}$  show rating  $j^{\text{th}}$  class is the class of the  $i^{\text{th}}$  that are rated and weighted [20].

#### 3.2. Fuzzy logic Method

In a Fuzzy Map, the associated value for each pixel (Fuzzy Membership Value), represents both the relative importance of the factors and the relative values corresponding to different locations on the map. Fuzzy Membership Values should be between zero and one. However, in this range, there is no limit on the selection of the values. They are selected to represent the degree of membership in a set on the basis of subjective judgment. In fact, each membership value represents the suitability of the pixel area for the power station with regard to the related criteria [23,24].

The Fuzzy Logic method was established by [25] and is used in many cases where it is not possible to make a decision on the existence or nonexistence of a certain phenomenon, thus a gradual boundary exists. This method contains functions that can be used in making decisions [9,26]. Five Fuzzy operators namely Fuzzy Subscription, Gathering Fuzzy, Multiplication Fuzzy and Gamma Fuzzy Complex use a combination of factors for data integration [27-30]. Several Fuzzy operators (Fuzzy AND, Fuzzy OR, Fuzzy Algebraic Sum, Fuzzy Algebraic Product and Fuzzy Gamma) allow the flexible combination of input maps (instability factor maps) in a series of steps. In this analysis Fuzzy Gamma is used. The Fuzzy Algebraic sum and the Fuzzy Algebraic product were calculated and combined using the Fuzzy Gamma Operator [3].



**Legend**

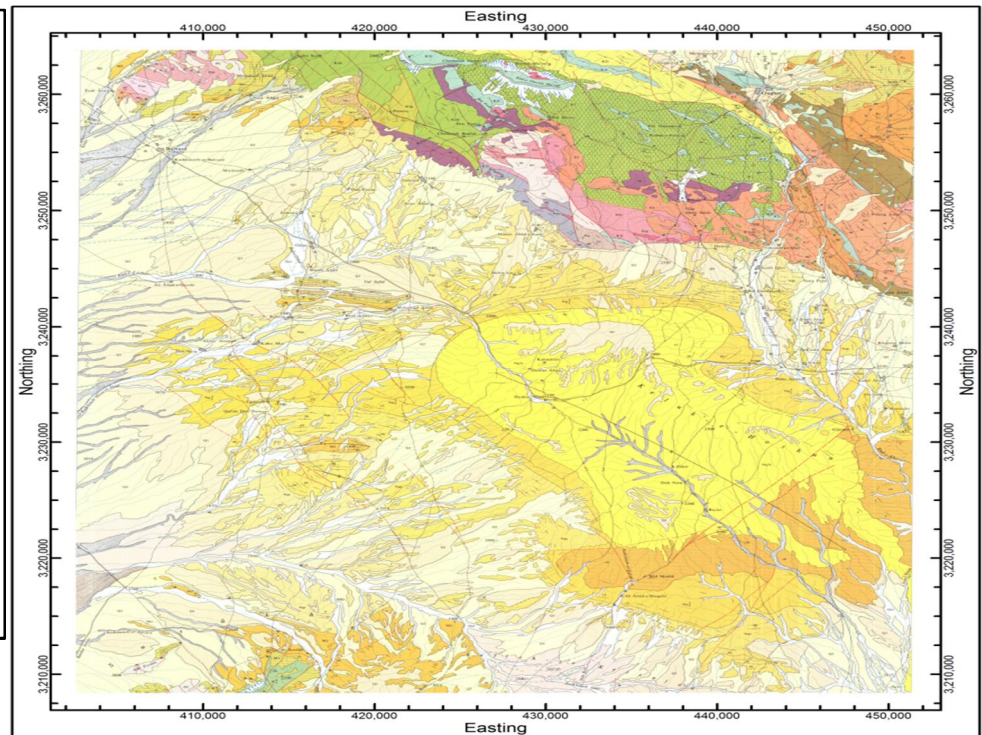
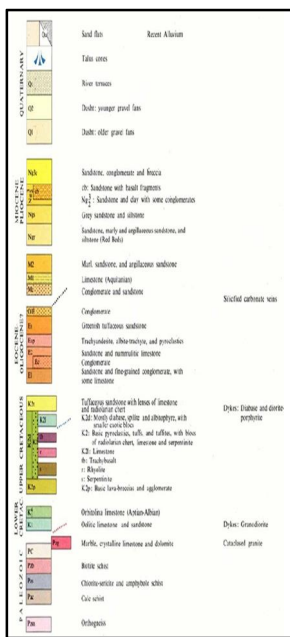


Fig. 2. Geological map of Balvard 1:100,000 sheet within the Nain-Baftophiolites in the Sanandaj-Sirjan structural-metamorphic zone [14].

**3.2.1. Fuzzy AND**

This is equivalent to a Boolean AND (logical intersection) operation on classical set values of (1, 0). It is defined:

$$\mu_{\text{Combination } A B C} = \text{MIN}(\mu_A, \mu_B, \mu_C, \dots)$$

Where  $\mu_A$  is the membership value for map A at a particular location:  $\mu_B$ , is the value for map B, and so on. Of course, the Fuzzy memberships must all be with respect to the same proposition. Suppose that at some location the membership value for map A is 0.75 and

for map B is 0.5, then the membership for the combination using Fuzzy AND is 0.5. It can readily be seen that the effect of this rule is to make the output map be controlled by the smallest Fuzzy membership value occurring at each location. Like the Boolean AND, Fuzzy AND results in a conservative estimate of set membership, with a tendency to produce small values. The AND operation is appropriate where two or more pieces of evidence for a hypothesis must be present together for the hypothesis to be true.

### 3.2.2. Fuzzy OR

On the other hand, the Fuzzy OR is like the Boolean OR (logical union) in that the output membership values are controlled by the maximum values of any of the input maps, for any particular location. The Fuzzy OR is defined as:

$$\mu_{\text{Combination } A B C} = \text{MAX}(\mu_A, \mu_B, \mu_C, \dots)$$

Using this operator, the combined membership value at a location (=suitability for landfill etc) is limited only by the most suitable of the evidence maps. This is not a particularly desirable operator for the landfill case, but might in some circumstances be reasonable for mineral potential mapping, where favorable indicators of mineralization are rare and the presence of any positive evidence may be sufficient to suggest favorability. Note that in using either the Fuzzy AND or Fuzzy OR, a Fuzzy membership of a single piece of evidence controls the output value. On the other hand, the following operators combine the effects of two or more pieces of evidence in a "blended" result, so that each data source has some effect on the output.

### 3.2.3. Fuzzy Algebraic Product

Here, the combined membership function is defined as:

$$\mu_{\text{Combination}} = \prod_{i=1}^n \mu_i \quad (4)$$

Where  $\mu_i$  is the fuzzy membership function for the  $i$ -th map, and  $i = 1, 2 \dots n$  maps are to be combined. The combined Fuzzy membership values tend to be very small with this operator, due to the effect of multiplying several numbers less than 1. The output is always smaller than, or equal to, the smallest contributing membership value, and is therefore "decreasing".

### 3.2.4. Fuzzy Algebraic Sum

This operator is complementary to the Fuzzy Algebraic product, being defined as:

$$\mu_{\text{Combination}} = 1 - (\prod_{i=1}^n (1 - \mu_i)) \quad (5)$$

The result  $\mu_i$  is always larger (or equal to) the largest contributing Fuzzy membership value. The effect is therefore "increasing". Two pieces of evidence that both favor a hypothesis reinforce one another and the combined evidence is more supportive than either piece of evidence taken individually.

### 3.2.5. Gamma Operation

This is defined in terms of the Fuzzy Algebraic product and the Fuzzy Algebraic sum by = (Fuzzy Algebraic sum)

$$\mu_{\text{Combination}} = (\text{Sum})^\gamma \times (\text{Product})^{1-\gamma} \quad (6)$$

Where  $\gamma$  is a parameter chosen in the range (0, 1), [31]. When  $\gamma$  is 1, the combination is the same as the Fuzzy Algebraic sum; and when  $\gamma$  is 0, the combination equals the Fuzzy Algebraic product. Judicious choice of  $\gamma$  (produces output values that ensure a flexible compromise between the "increasing" tendencies of the

Fuzzy Algebraic sum and the "decreasing" effects of the Fuzzy Algebraic product.

Fuzzy Gamma is a compromise between the increasing tendencies of the Fuzzy Algebraic sum and the decreasing effect of the Fuzzy Algebraic product. With  $\gamma$  (gamma) the decreasing or increasing tendency can be controlled.  $\gamma$  (gamma) is a parameter chosen between 0 and 1. When  $\gamma$  is 1 the combination equals the Fuzzy Algebraic sum, when  $\gamma$  is 0 the combination equals the Fuzzy Algebraic product. An advantage of the Fuzzy Gamma operator is that different scenarios can be compared easily from the maps produced during the process.

## 4. Layers of exploratory data

The exploration layers were extracted from geological maps, remote sensing, geochemical and geophysical airborne data. They were divided into different classes after investigation and normalized in a range between 0-1. The layers were then combined using the mentioned methods.

### 4.1. Geological layers

Basic pyroclastic rocks, tuffs, limestones, serpentines and diabasic parts host the main mineralization of Fe and Mn in the area. Andesites and trachy-andesites contain low values of Fe and Mn mineralization in the area (Figure 3). The given weights of lithological units using the Index method and Fuzzy Logic are presented in Table 1. Geological weight units are according to the proper units for iron and manganese mineralization with expert perspective.

### 4.2. Structures Layers

Two major faults with trending of the NW-SE and NE-SW are located in the northern part of the area (Fig. 4). The mineralization occurred mostly at the intersection of the faults. The related weights are shown in Table 2.

#### 4.2.1. The weighting methods

##### 4.2.1.1. Ranking methods:

The simplest way to assign weights to the criteria is by arranging them according to the decision maker's comments. The criteria can be directly arranged (most important criterion=1, second criterion = 2 and ...) or reversely (least important criterion=1 and ...). Numerical weights must be calculated after arranging the criteria.

##### 4.2.1.2 Rating methods:

In these methods it is necessary for the decision maker to estimate the weight of the criteria on the basis of a predetermined scale. For example, a scale of 0 to 100 can be used. One of the simplest rating methods is Point Allocation.

Table 1. Weights of different members of the geological layer using two Indexes Overlay and Fuzzy Logic methods.

Weighted fuzzy logic method	Weighted index overlay method	Geological units
0.100000002 – 0.200000003	1	Sandstone and clay with some conglomerates
0.100000002 – 0.200000003	1	Sandstone, conglomerate and breccia
0.100000002 – 0.200000003	1	Sandstone with basalt fragments
0.100000002 – 0.200000003	1	Grey sandstone and siltstone
0.100000002 – 0.200000003	1	Sxpanse of sand
0.100000002 – 0.200000003	1	Grey sandstone and siltstone
0.100000002 – 0.200000003	1	Older gravel
0.100000002 – 0.200000003	1	Serpentinite
0.5 – 0.800000012	9	Limestone
0.200000003 – 0.5	4	Limestone nummolities
0.100000002 – 0.200000003	2	Sandstone and fine-grained conglomerate with areas of limestone
0.200000003 – 0.5	5	Conglomerate
0.100000002 – 0.200000003	1	Young gravels
0.800000012-0.899999976	10	Basic pyroclastic rocks, tuffs, tuffits, with masses of radiolarites Chert, limestone and serpentine
0.200000003 – 0.5	3	Calk-schist
0.200000003 – 0.5	4	Limestone nummolities
0.5 – 0.800000012	8	Trachy-basalt
0.200000003 – 0.5	3	Chlorite-sericite and amphibole-schist
0.200000003 – 0.5	5	Biotitic schist
0.100000002 – 0.200000003	2	Sandstone and fine-grained conglomerate with areas of limestone
0.200000003 – 0.5	5	Marble, crystalline limestone and dolomite
0.100000002 – 0.200000003	2	Sandstone, marly and argillaceous sandstone and siltstone (Red Beds)
0.100000002 – 0.200000003	2	Conglomerate and sandstone
0.100000002 – 0.200000003	1	Expanse of sand
0.100000002 – 0.200000003	1	Limestone (Aquitania)
0.100000002 – 0.200000003	2	Marl, sandstone, and argillaceous sandstone
0.200000003 – 0.5	5	Shear basic lava and agglomerate
0.5 – 0.800000012	8	Most diabase, split and albitofir with smaller output components
0.200000003 – 0.5	4	Green tuff sandstone

In this method the decision maker is asked to divide 100 scores among the various criteria between 0 and 100. A score of 0 is given to the criterion that can be ignored while a score of 100 is given to the criterion that should be most highly considered. A higher scored criterion indicates a higher relative importance of that criterion in comparison with the other criteria.

#### 4.3. Alterations layer

Distribution of alteration zones is one of the important

parameters for exploration of magmatic, metamorphic and hydrothermal deposits. The alterations associated with iron and manganese mineralization consist of iron oxide and hydroxide (jarosite, hematite, limonite and goethite), serpentinite, propylitic (epidote and chlorite), argillic (kaolinite and Montmorillonite) and carbonate (calcite and dolomite) using ASTER and ETM<sup>+</sup> which were obtained using the MF (Match Filtering) method (Fig. 5: [32]). The related weights are indicated in Table 3.

Table 2. Weight of the fault layers using two methods, Indexes Overlay and Fuzzy Logic.

Weighted fuzzy logic method	Weighted index overlay method	Faults
0.100000002	10	Main
0.100000002-0.600000024	5	Subsidiary
0.600000024-0.899999976	0	Others

Table 3. Weights associated with each alteration using the two methods, Index Overlay and Fuzzy Logic.

Weighted fuzzy logic method	Weighted index overlay method	Alterations
0.899999976 -0	1	argillic
0.899999976 -0	1	Serpentinite
0.899999976 -0	1	carbonate
0.899999976 -0	1	propylitic
0.899999976 -0	1	iron oxide

#### 4.4. Geochemical Layers Using C-N Fractal Modeling

[33] defines a fractal distribution as the number of objects  $N$  with a size [34] greater than  $r$  scales and the relationship between the desired certain attributes (e.g., ore element) and the cumulative number of samples of those attributes. [35] proposes a grade-size multifractal model for giant and supergiant deposits. It is revealed that element enrichment can result in a fractal distribution. The N-S fractal model is used to describe the distribution of elements without pre-treatment and evaluation of data [36]. The model is expressed by the following equation:

$$N(\geq \rho) \propto \rho^{-\beta} \quad (7)$$

Based on [36], it also can be rewritten as

$$\text{Log}[N(\geq \rho)] = -\beta \text{log}(\rho) \quad (8)$$

Where  $\rho$  denotes the element concentration,  $N(\geq \rho)$  is the cumulative sample number with concentration values equal to or greater than the concentration value ( $\rho$ ), while  $\beta$  is the scaling exponent or fractal dimension of the concentration distribution. Frequency distributions of elements displayed in log-log plots show the logarithm of the cumulative number of samples exceeding a certain element concentration plotted against the logarithm of the element concentration [38]. Straight lines in the log-log plots have the slopes  $-\beta$  within different concentration intervals [36].

Based on the stream sediment data, the C-N log-log plots were generated for Fe and Mn (Fig. 6). Break points between straight-line segments in those log-log plots indicate threshold values for separating populations of geochemical concentration values representing geological differences due to distinct

geochemical processes. Based on the log-log plot, there are five populations for Fe and four populations for Mn, as depicted in Fig. 6. The first and high intensity anomalies thresholds for Mn are 1023 and 1585 ppm, respectively (Fig. 6). The first threshold for Fe is 3.3% and high intensity anomaly starts at 6.9 % (Fig. 6). The Fe log-log plot shows a major Fe enrichment started at 6.9 %. Geochemical maps of the first and final factors were created by RockWorks™ 15 software package. Based upon the results of the C-N method, elemental distribution maps were built up (Fig. 7). According to the mapping of the C-N fractal modeling results for the elements, the main anomalies of Mn and Fe occurred in the central and northern parts of the region, as shown in Fig. 7.

#### 4.5. Geophysics Layer

Airborne magnetic survey techniques are a practical and important method in the exploration of iron ore. The high intensive anomalies of total magnetic are situated in the northern area, especially the northeastern portion of the studied area (Fig. 8).

### 5. Combining the informative layers

#### 5.1. Index Overlay

In this method every layer, according to the values of their units, is given various classes. Additionally, every layer has an especial weight based on studies and expert opinion (Table 4). After processing, the potential target map of iron and manganese is prepared using the Index Overlay method (Fig. 9). In the northern areas a priority of 6 and 5, using red and green respectively, show the best areas for the prospecting and exploration of iron and manganese (Fig.9).

The following equation was used for the calculation of cells' values based on index overlay:

$$\text{Formula} = [(\text{Geochemical anomaly} \times 30) + (\text{Magnetometry} \times 20) + (\text{Lithology of Fe} \times 15) + (\text{iron oxide} \times 10) + (\text{fault} \times 10) + (\text{propylitic} \times 5)) + (\text{Lithology of Mn} \times 5) + (\text{argillic} \times 3)) + (\text{Carbonate} \times 2)] / 100 \quad (9)$$

Table 4. Weights of exploration layers in the Index Overlay method

Layers	Weight
Geochemical anomaly	30
Magnetometry	20
Lithology of Fe	15
Iron oxide	10
fault	10
Propylitic	5
Lithology of Mn	5
Argillic	3
Carbonate	2

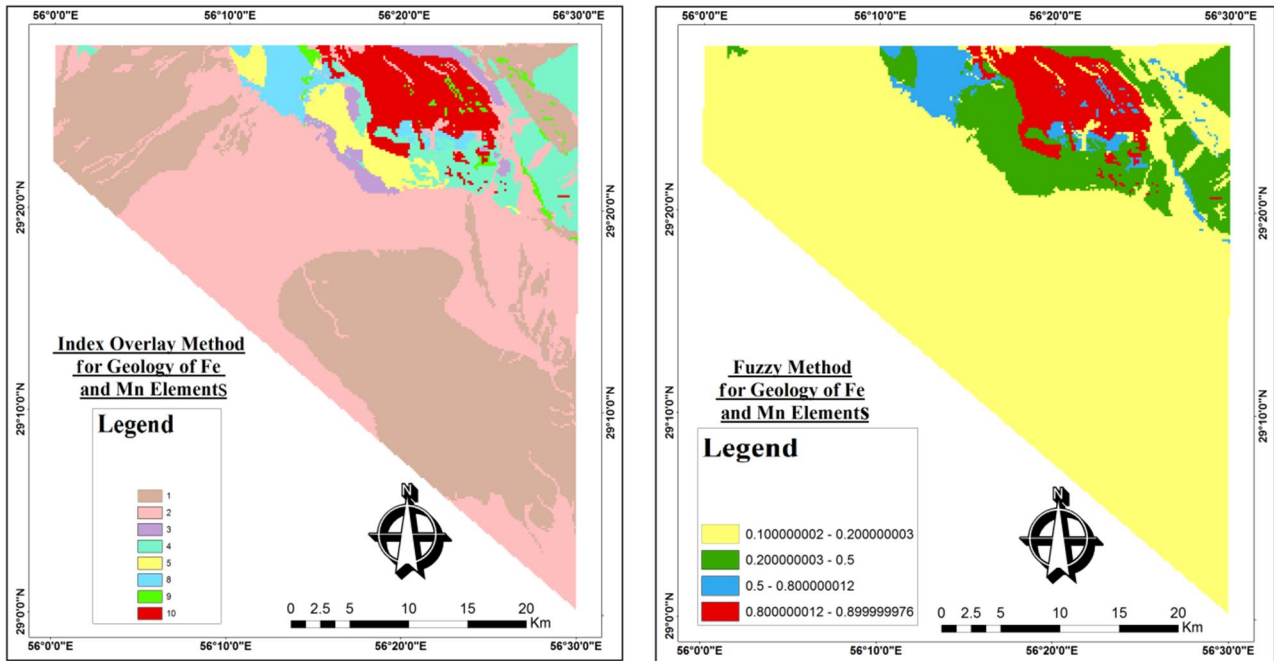


Fig. 3. Layers of geological units using index Overlay and Fuzzy Logic methods

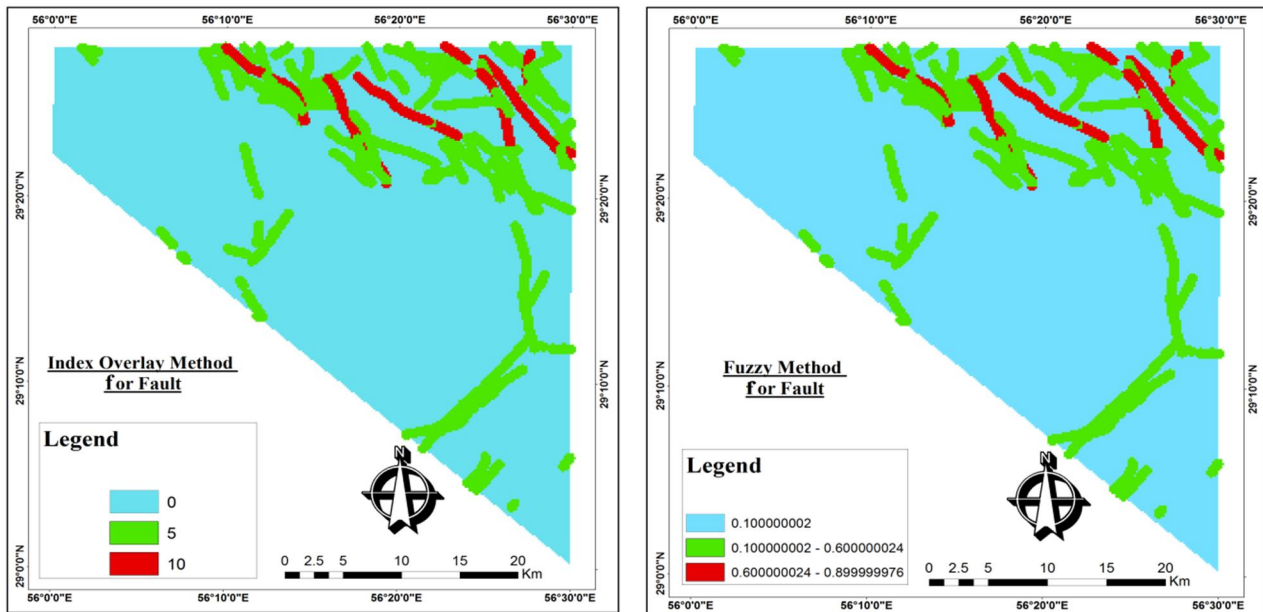


Fig.4. Fault layer, using index Overlay and Fuzzy Logic methods

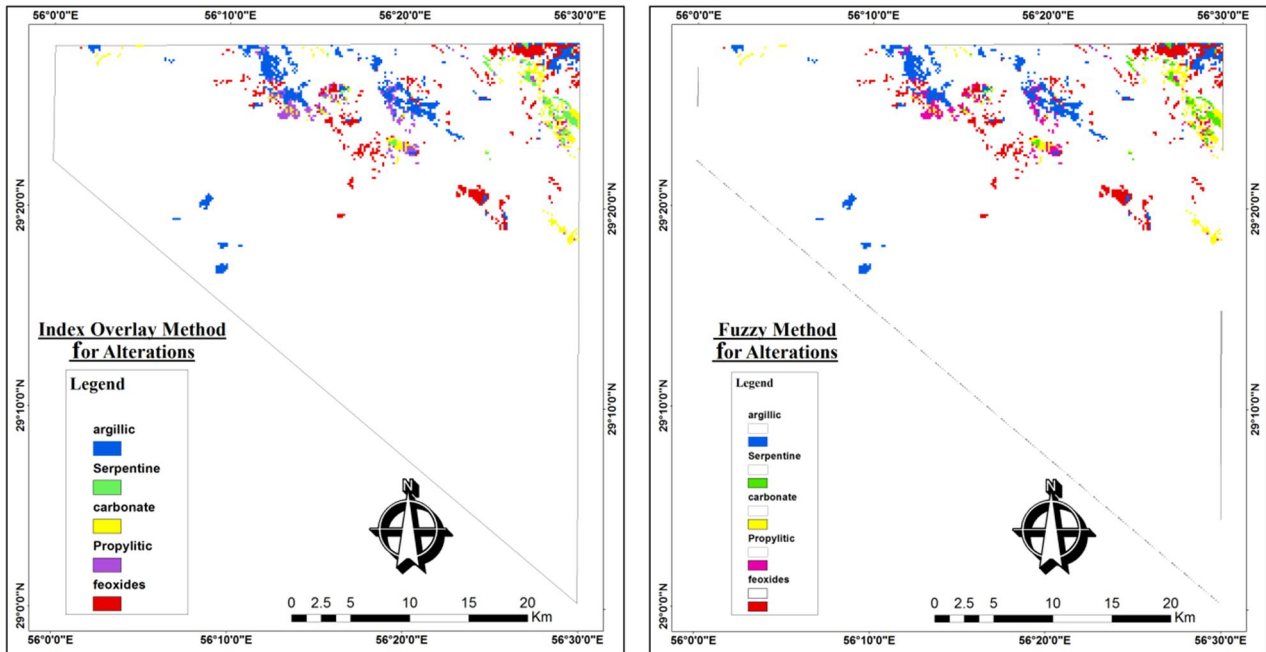


Fig.5. Layers of alterations using Index Overlay and Fuzzy Logic methods

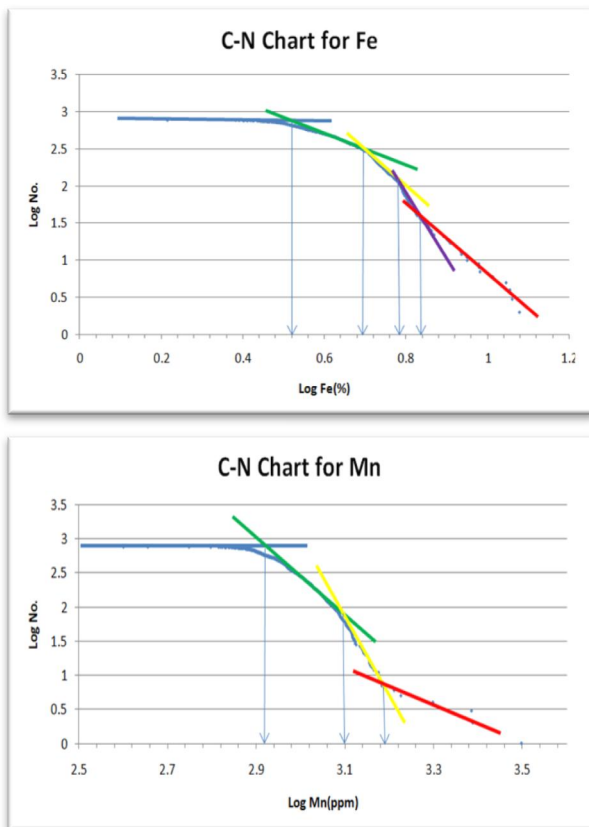


Fig. 6. C–N log–log plots for Fe and Mn

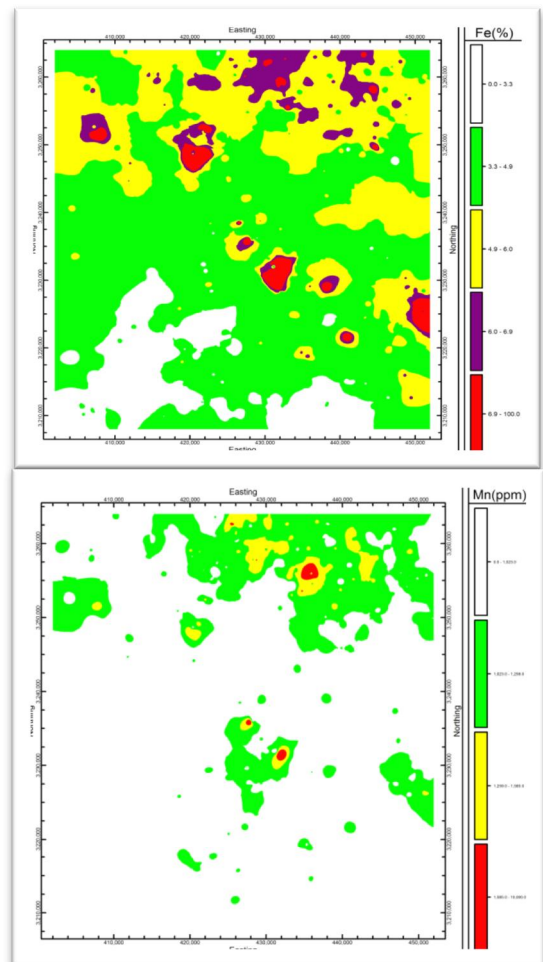


Fig.7. Fe and Mn geochemical distribution maps based on the C–N model



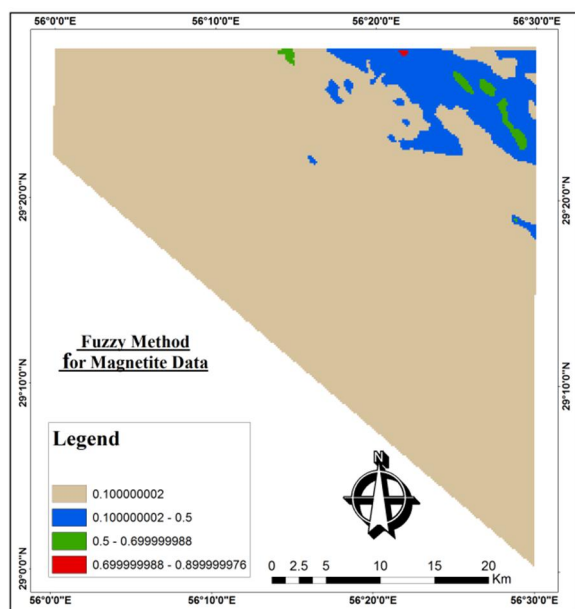
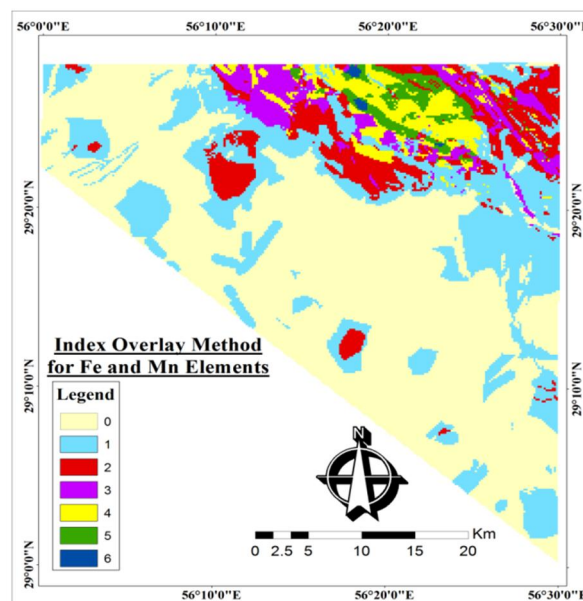
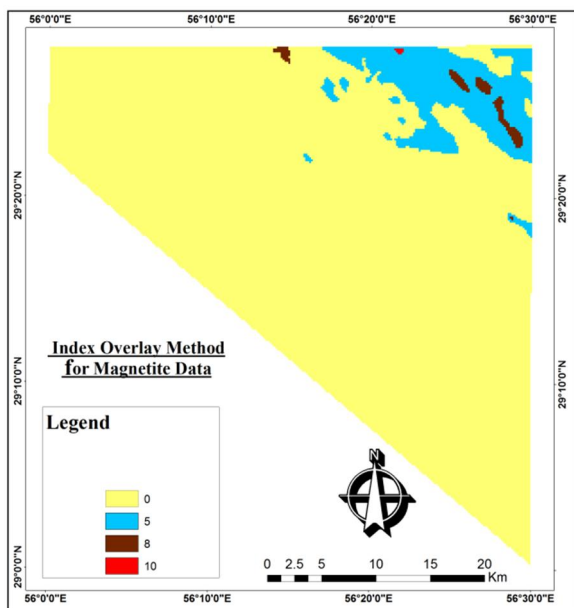


Fig.8. Distribution of magnetic intensity using Index Overlay and Fuzzy Logic method (The red portion indicates the main area of detailed exploration).

Fig.9. Map of iron, and manganese prospects using the Index Overlay method with weighted coefficient for total layers. The method of index overlay is based on categories integers. Priority six (6) represents the best area for the prospecting of iron and manganese in the study area.

### 5.2. Fuzzy logic

In this method, as in the Index Overlay method, for each factor map we can define classes. Based on previous studies and expert opinion, first SUM and OR operation and then  $\gamma$  equals 0.75 were used (Fig. 10). After processing, the map of iron and manganese prospects was prepared using the Fuzzy Logic method (Fig. 11). The northern and northeastern portions of the studied area shown using dark blue are the best areas for iron and manganese mineralizations. Using this method the suitable areas for iron and manganese mineralization are larger than the Index Overlay method.

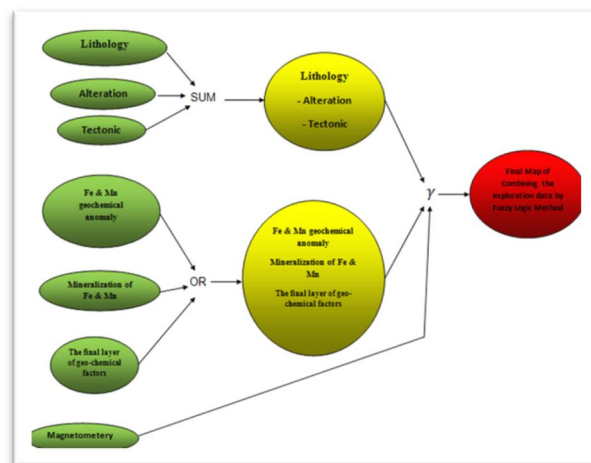


Fig.10. Flowchart of the analysis performed on the exploration layers using the Fuzzy Logic method.

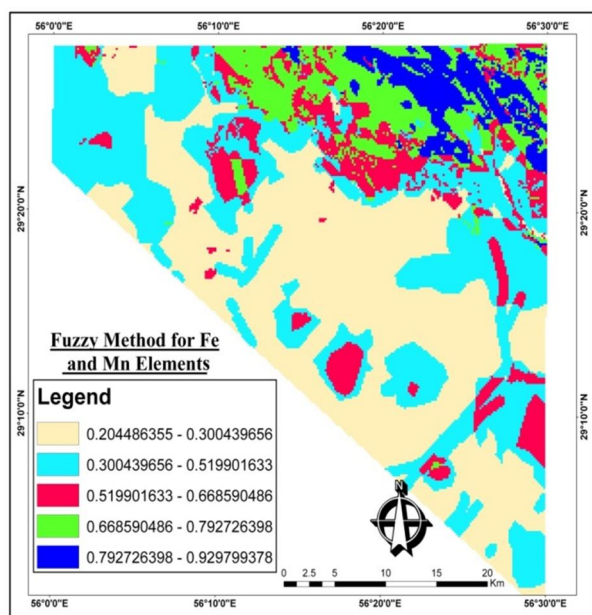


Fig. 11. Map of the iron and manganese prospects using the Fuzzy Logic method.

## 6. Conclusions

In this study, the maps of the study areas show prospects for Fe and Mn mineralization. These maps were obtained using GIS modeling with Indexing Overlay and Fuzzy Logic methods for the introduction of appropriate areas of Fe and Mn mineralization. Based on the results obtained from both methods, the northern and northeastern parts of the Balvard area showed Fe and Mn prospects which correlated with ultramafic units and faults. Comparison between the methods indicated that the prospects derived via the Fuzzy Logic method were more extensive than the prospects obtained from the Index Overlay method. Results using Fuzzy Logic provided an area larger than those of Index Overlay because the method used was in the range from 0 to 1 value. This shows that Fuzzy Logic is actually a developed form of Boolean Logic. In Fuzzy Logic, membership degree of a unit in a set is defined between one (full membership) and zero (not full membership). Thus the probability of error decreases and the weight is closer to reality. In this research, Fuzzy Factor Maps were created so that their pixel value would be distinctive and therefore show their relative importance in each class of the factor maps as well as the relative importance of each factor map.

## References

- [1] Carranza, E.J.M., 2008. Geochemical anomaly and mineral prospectivity mapping in GIS, Handbook of exploration and environmental geochemistry, vol 11. Elsevier, Amsterdam.
- [2] Pazand, K., Hezarkhani, A., Ghanbari, Y., 2012. Fuzzy analytical hierarchy process and GIS for predictive Cu porphyry potential mapping: a case study in Ahar–Arasbaran Zone (NW, Iran), Arabian Journal of Geosciences (In press).
- [3] Bonham-Carter, G.F., 1994. Geographic Information Systems for Geoscientists: Modelling with GIS, Pergamon Press, Oxford, 398 p.
- [4] Malczewski, J., 1999. GIS and multicriteria decision analysis, published in Canada and printed in USA, 392p.
- [5] Chattopadhyay, A., Holdsworth, R. E., McCaffrey, K. J. W., Wilson, R.W., 2010. Recording and analyzing geospatially accurate structural data through ‘digital mapping’ technique: A case study from the Canisp Shear Zone, NW Scotland. Journal of the Geological Society of India 75, 43-59.
- [6] Tamma Rao, G., Gurunadha Rao, V. V. S., Dakate, R., Mallikharjuna Rao, S. T., Raja Rao, B. M., 2012. Remote sensing and GIS based comparative morphometric study of two sub-watersheds of different physiographic conditions, West Godavari District, A.P. Journal of the Geological Society of India 79, 383-390.
- [7] Porwal, A., Carranza, E., and Hale, M., 2003. Knowledge-driven and Data-driven Fuzzy Models for Predictive Mineral Potential Mapping, Natural Resources Research 12(1), 1–25.
- [8] Pirmoradi, A., Vaezi, H., Baktash, P., Amiri, A., 2012. Role of SDI in index overlay Modeling and fuzzy logic in GIS to predict Malaria outbreak. Canada, Proceedings of Global Geospatial Conference 2012 Québec City, 14-17.
- [9] Yousefifar, S., Khakzad, A., Asadiharooni, H., Karami, J., Jafari, M.R., Vosoughiabedin, M., 2011. Prospecting of Au and Cu bearing targets by Exploration data Combination in Southern part of dalli Cu-Au Porphyry Deposit, Central Iran, Arch. Min. Sci 56, 21-34.
- [10] Taleb-Ouibrahim, Z.O., Benali, H., Medini, S., Belmouhoub, A., 2013. Developing a geographic information system (GIS) for mapping and analyzing the polymetallic deposits of M’Sirda volcanic province, Northwest Algeria, Arabian Journal of Geosciences (In press).
- [11] Azizi, H., Asaharab, Y., Mehrabic, B., Sun Lin Chungd., 2011. Geochronological and geochemical constraints on the petrogenesis of high-K granite from the Suffiabad area, Sanandaj-Sirjan Zone, NW Iran, Chemie der Erde 71, 363–376.
- [12] Sepahi, A.A., Jafari, S.R., Mani-Kashani, S., 2009. Low pressure migmatites from the Sanandaj-Sirjan Metamorphic Belt in the Hamedan region (Iran), Ggeol. Geol. Carpathica 60, 107–119.
- [13] Mehdipour Ghazi, J., Moazen, M., Rahgoshay, M., Moghadam, H., 2012. Geochemical characteristics of basaltic rocks from the Nain ophiolite (Central Iran); constraints on mantle wedge source evolution in an oceanic back arc basin and a geodynamical model, Tectonophysics 575, 92-104.
- [14] Moghadam, H., Whitechurch, H., Rahgoshay, M., Monsef, I., 2009. Significance of Nain-Baftophiolitic belt (Iran): Short-lived, transtensional Cretaceous back-arc oceanic basins over the Tethyan subduction zone. C. R. Geosci. 341: 1016–1028.
- [15] Moghadam, H., Stern, R.J., Chiaradia, M., Rahgoshay, M., 2013. Geochemistry and tectonic evolution of the Lte

- Cretaceous Gogher-Baftophiolite, Central Iran, Lithos 169, 33-47.
- [16] Sridic, A., Dimitrijevic, M.N., Cvetic, S., Dimitrijevic, M.D., 1972. Geological Map of Baft (1:100,000), Geological Survey of Iran.
- [17] Stocklin, J., Nabavi, M.H., 1972. 1/2,500,000 sheet, tectonic map of Iran. Geological Survey of Iran.
- [18] Aronof, S., 1989. Geographic Information Systems: A Management Perspective, Ottawa, Canada, WDL Publications.
- [19] Bonham Carter and G.F., 1991. Geographic Information System for Geoscientists: Modeling with GIS, Pergamon, Ontario, 319-470.
- [20] Malczewski, J., 2006. Ordered weighted averaging with fuzzy quantifiers: GIS-based multicriteria evaluation for land-use suitability analysis, International Journal of Applied Earth Observation and Geo information 8(4), 270-277.
- [21] Noorollahi, Y., Itoi, R., Fujii, H., Tanaka, T., 2007. GIS integration model for geothermal exploration and well siting, Geothermics 37, 107-131.
- [22] Sadeghi, B., Noorollahi, Y., Radan, M.Y., Khalajmasoumi, M., 2013. Evaluation of geothermal potentials using Index Overlay and Fuzzy Logic methods, Eastern Azarbayegan province 1:250,000 mapping sheet, Journal of Earth and Resources 18, (In press).
- [23] Chi, K. H., Park, N. W., Chung, Ch.J., 2001. Fuzzy Logic Integration for Landslide Hazard Mapping Using Spatial Data from Boeun, Korea 3, 87-95.
- [24] Shahabi, H., Allahvirdiasl, H., Ali zadeh, M., 2012. Application of GIS Models in Site selection of waste disposal in Urban Area, IOSR Journal of Applied Physics (IOSRJAP) 1, 01-07.
- [25] Zadeh, L.A., 1965. Fuzzy sets, Inf Control 8(3), 338-353.
- [26] Ouenes A., 2000. Practical application of fuzzy logic and neural networks to fractured reservoir characterization. Computers & Geosciences 26(8), 953-962.
- [27] Fisher, P. F., 1989. Knowledge-based Approaches to Determining and Correcting Areas of Unreliability in Geographic Databases, Goodchild, M., Gopal, S.: The Accuracy of Spatial Databases (45-54), Taylor & Francis, London, 45-54.
- [28] Zimmermann, H. J., 2001. Fuzzy Set Theory and Its Applications. 4<sup>th</sup> Ed. Kluwer Academic Publishers, Dodrecht, London.
- [29] Hansen, H. S., 2003. "A Fuzzy Logic Approach to Urban Land-use Mapping." Proc., Scan-GIS 2003, Helsinki, Denmark, 1-10.
- [30] Menhaj, M. B., 2007. Fuzzy computing. 1<sup>st</sup> Ed. Amirkabir Pub., Tehran, Iran, Modeling of Needs for Industry and Mine Ministry, MSc thesis (in Persian with English abstract), Engineering Faculty, Khajeh Nasir Toosi University (KNTU), Tehran, Iran.
- [31] Zimmermann, H.-J., Zysno, P., 1980. Decisions and evaluations by hierarchical aggregation of information, Fuzzy Sets and Systems 4, 37-51.
- [32] Sadeghi, B., Khalajmasoumi, M., Afzal, P., Moarefvand, P., Yarebi, A.B., Wetherelt, A., Foster, P., Ziazarifi, A., 2013. Using ETM<sup>+</sup> and ASTER sensors to identify iron occurrences in the Esfordi 1:100000 mapping sheet of Central Iran, Journal of African Earth Sciences 85, 103-114.
- [33] Mandelbrot B.B., 1983. The Fractal Geometry of Nature: W. H. Freeman. San Fransisco, 468 p.
- [34] Mohammadi, A., Khakzad, A., Rashidnejad Omran, N., Mahvi, M.R., Moarefvand, P., Afzal, P., 2013. Application of number-size (N-S) fractal model for separation of mineralized zones in Dareh-Ashki gold deposit, Muteh Complex, Central Iran. Arabian Journal of Geosciences 6: 4387-4398.
- [35] Agterberg F.P., 1995. Multifractal modeling of the sizes and grades of giant and supergiant deposits, International Geology Review 37, 1-8.
- [36] Deng J., Wang Q., Yang L., Wang Y., Gong Q., Liu H., 2010. Delineation and explanation of geochemical anomalies using fractal models in the Heqing area, Yunnan Province, China.
- [37] Zuo, R., Cheng, Q., Xia Q., 2009. Application of fractal models to characterization of vertical distribution of geochemical element concentration. Journal of Geochemical Exploration 102 (1), 37-43.
- [38] Monecke, T., Monecke, J., Herzi, P.M., Gemmel J.B., Monch W., 2005. Truncated fractal frequency distribution of element abundance data: A dynamic model for the metasomatic enrichment of base and precious metals, Earth and Planetary Science Letters 232, 363-378.